CrystEngComm

PAPER

View Article Online
View Journal | View Issue

Cite this: *CrystEngComm*, 2024, **26**, 4643

Amidinium···phosphonate charge assisted hydrogen-bonded organic frameworks: influence of diverse intermolecular interactions†

Asia R. Y. Almuhana,[ab] Sarah L. Griffin[b] and Neil R. Champness *[b]

Received 13th May 2024,
Accepted 17th July 2024

DOI: 10.1039/d4ce00479e

rsc.li/crystengcomm

The synthesis of charge assisted amidinium···phosphonate hydrogen-bonded organic frameworks (HOFs) is reported. Two tectons, with either a biphenyl or naphthalene diimide backbone, were combined with bis-amidinium salts to afford **HOF1** and **HOF2**, respectively. Whereas **HOF1** formed rapidly, typically within two days of mixing, **HOF2** proved more challenging to synthesise. Interestingly, the presence of sunlight facilitated the rapid formation of **HOF2** within a few hours. Although crystals of tectons $\mathbf{1}H_4$ or $\mathbf{2}Et_4$ exhibited densely packed structures, combination of the corresponding phosphonate bases with bis-amidinium cations, through amidinium···phosphonate interactions, gave open framework materials. The HOFs formed through this approach exhibited notable stability limitations, including a propensity for phase transformations or structural collapse upon solvent removal.

Introduction

Crystal engineering and supramolecular chemistry employ the ability of intermolecular interactions to organise the arrangement of molecules with respect to one another.[1,2] This simple concept is illustrated by the archetypal supramolecular synthon – the hydrogen bond. In the solid-state hydrogen bonds can be used to organise molecules in three-dimensional space to prepare framework structures which have become known as hydrogen-bonded organic frameworks or HOFs.[3–7] Tuning the structure of the molecular components, or tectons, and choice of the supramolecular synthons, or intermolecular interactions, can be used to direct the nature of the resulting self-assembled structure.[2,8,9] Within the many factors that influence self-assembly the nature of the hydrogen bond donor and acceptor is perhaps paramount, accompanied by tecton geometry and conformational flexibility. Variation of these factors yield a distinct fingerprint of the self-assembly processes.

Charge-assisted hydrogen bonds have been shown to be an effective approach to creating HOFs, notably using the interaction between bis-amidinium cations and carboxylate anions.[10–14] In this study we demonstrate how this strategy can be modified to employ a charge-assisted supramolecular synthon adopted between bis-phosphonate anions and bis-amidinium cations. To our knowledge previous reports of the amidinium···phosphonate synthon being used for HOF formation are relatively unusual,[15,16] particularly in comparison to corresponding amidinium···carboxylate systems.[10–14] Notably, anti-electrostatic hydrogen bonds have been employed using phosphonate anions, providing an alternative strategy to incorporating phosphonate into self-assembled structures.[17,18]

In this study two distinct backbones are used for the bis-phosphonate tecton, biphenyl and naphthalene diimide (NDI), which afford distinct structural properties allowing us to draw comparisons between related HOFs. Thus, we demonstrate that when combined with amidinium tectons, these phosphonate anions engage in a diverse range of intermolecular hydrogen bonding interactions, resulting in the formation of extended framework structures.

Results and discussion

As noted above we wish to explore the range of HOFs that could be prepared using the amidinium···phosphonate synthon and to demonstrate the utility of this supramolecular synthon.

A biphenyl-4,4′-diphosphonate **1** was selected as the first anionic tecton. **1** has been used previously as a ligand for MOF synthesis, including examples that exhibit increased quantum yields or moisture stability.[19–23] $\mathbf{1}H_4$ consists of a rigid centre linked to flexible phosphonate moieties *via* methylene groups. It has previously been suggested that the more flexible the tecton, the more readily it can adapt to form hydrogen bonds, thus facilitating the growth of co-crystals,[24] and by analogy HOFs. The phosphonate groups tend to pack densely, resulting in layered structures without pores; however, it is

[a] *King Faisal University, P.O. 380, Al-Ahsa 31982, Saudi Arabia*
[b] *School of Chemistry, The University of Birmingham, Birmingham, UK. E-mail: n.champness@bham.ac.uk*

† Electronic supplementary information (ESI) available: CCDC 2352949–2352952. For ESI and crystallographic data in CIF or other electronic format see DOI: https://doi.org/10.1039/d4ce00479e

anticipated that using a secondary tecton to form a HOF could facilitate the construction of porous structures.

Rylene diimides are interesting examples of tectons for HOF formation,[14,25] due to their redox and photochemical activity, as well as high thermal and chemical stability.[26] Indeed, we have recently reported the synthesis and photoinduced radical formation in a NDI-containing HOF constructed using amidinium···carboxylate synthons.[14] The rich chemistry of NDIs means they are readily functionalized with a variety of moieties,[27] enabling the introduction of a variety of hydrogen-bonding sites, making them ideal tecton candidates for HOF formation.

Synthesis and structures

$\mathbf{1}H_4$ was synthesised from tetraethyl biphenyl-4,4′-diphosphonate by hydrolysis with 6 M HCl. The NDI-based anion was synthesised in a two-step process. Firstly, $\mathbf{2(Et)_4}$, was prepared *via* a straightforward condensation reaction between diethyl 4-aminobenzylphosphonate and 1,4,5,8-naphthalene dianhydride. This compound exhibited notable solubility in a wide range of organic solvents. The anion, $\mathbf{3}^{4-}$, was prepared by de-esterification using trimethylsilyl bromide and the subsequent acid deprotonated to form the bisphosphonate species. The two bisphosphonate species, which are soluble in water, have the ability to establish charge-assisted hydrogen bonds with amidinium donors and hence can form dual-component HOFs.

Single crystals of $\mathbf{1}H_4$ were grown from a water and MeOH mixture, whereas colourless needle-shaped single crystals of $\mathbf{2(Et)_4}$ were grown *via* slow evaporation of a solution of the compound in CH_2Cl_2. The crystal structures of these two tectons allows the determination of the conformational arrangement of the molecules in the solid state (Fig. 1). The structure of $\mathbf{1}H_4$ reveals a co-planar arrangement of the biphenyl unit and a transoid configuration of the two phosphonate groups. In the case of $\mathbf{2(Et)_4}$ the two phenyl groups attached to the imide groups adopt an angle of 70.12° with respect to the plane of the NDI, and the phosphonates, once again, adopt a transoid arrangement.

Crystals of **HOF1** were grown by layering an aqueous solution of 1,4-phenyl-bis-amidinium dichloride over an aqueous solution of $\mathbf{1}H_4$, containing two drops of 1 M NaOH to deprotonate the acid. The two layers were separated by 1 mL of MeOH in order to slow the crystallization process. Colourless needle crystals were formed which were of suitable quality for analysis by single crystal X-ray diffraction (SCXRD). The crystal structure of **HOF1** reveals that the anion was partially deprotonated, releasing two of the four protons, to form $\mathbf{1}H_2^{2-}$. Thus, each phosphonate group presents two hydrogen bond acceptors and one donor, enabling the anionic components to interact with each other by hydrogen bonds, as well as interacting with bis-amidinium cations. The anionic and cationic tectons pack in a layered arrangement, with a layer of cations followed by an anion layer (Fig. 2a). This results in a sheet-like structure with pores that encapsulate two water molecules. The biphenyl group is

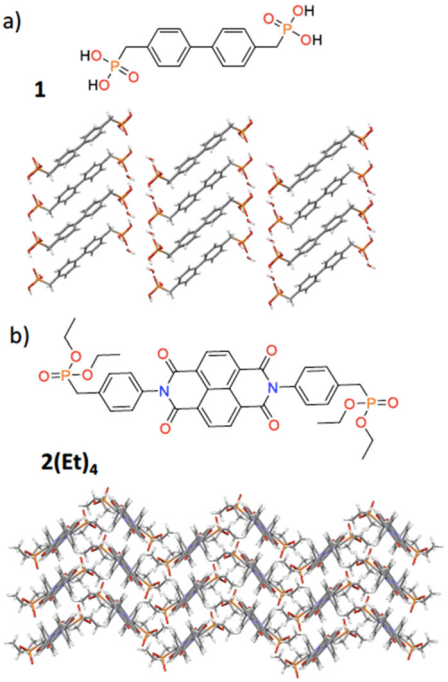

Fig. 1 Compounds a) $\mathbf{1}H_4$ and b) $\mathbf{2(Et_4}$ accompanied by views of their single crystal structures viewed along the *b*-axis and *c*-axis respectively.

buckled in the $\mathbf{1}H_2^{2-}$ tectons (14.2° interplanar angle between phenyls) and the phosphonate groups are arranged in a cisoid fashion, in contrast to the free tecton (see above), leading to an extensive network of interactions formed between cations and anions, with each $\mathbf{1}H_2^{2-}$ tecton interacting with four adjacent bis-amidinium cations (Fig. 3). Each phosphonate group interacts with two bis-amidinium cations, one through two parallel O···H–N interactions (d_2a_2), and the other through a single hydrogen bond (d_1a_1).

The ability of **HOF1** to survive solvent removal was evaluated by powder X-ray diffraction (PXRD) studies revealing that air-dried crystals lose crystallinity. Notably **HOF1** showed no evidence of π-based interactions which might be anticipated to provide additional stability to the framework. Therefore, it was decided to explore a tecton with a larger aromatic surface, **3**.

Crystals of **HOF2** were formed using a layering approach at room temperature (*ca.* 25–27 °C) in the presence of sunlight. After 5 hours of diffusion, long yellow needle crystals (**HOF2**) were formed (Fig. 4a). The crystallisation process was sensitive to sunlight and temperature. Indeed, the crystallisation process was found to be highly irreducible and was extremely sensitive to the laboratory environment, simply changing laboratory made attempts at crystal growth unsuccessful. The use of light to grow crystals is a common technique for growing amino acid crystals.[22–24] Light may also be used to control monomer self-assembly and facilitate crystallization by modifying the solubility of molecules after irradiation.[28–30] Notably this has previously been demonstrated for the crystallisation of an amidinium···carboxylate based HOF.[31] In the study by White *et al.*, light is believed to control tecton release for self-assembly

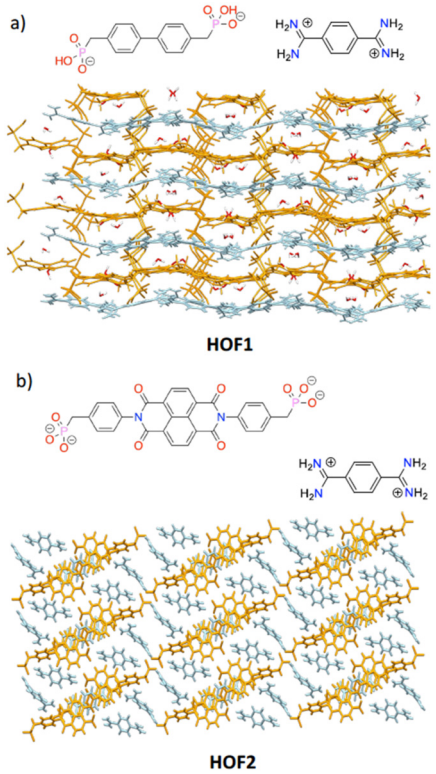

Fig. 2 Views of the crystal structures of a) **HOF1** and b) **HOF2** both viewed along the *a*-axis. In these figures, the gold-coloured structure represents the phosphonate-containing anion tecton, while the blue structure represents the bis-amidinium component. In a) guest H_2O molecules are shown in red.

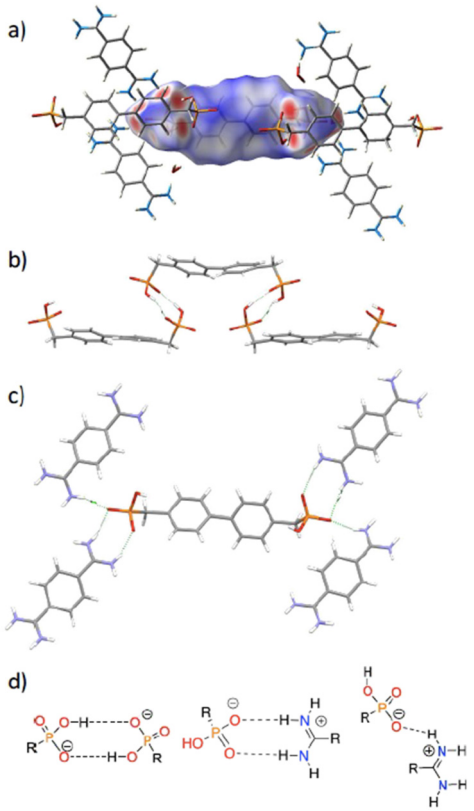

Fig. 3 **HOF1**: a) d_{norm} surface showing molecules in close proximity to $\mathbf{1}H_2^{2-}$ in **HOF1** (represented by red spots); b) H-bond interactions between $\mathbf{1}H_2^{2-}$ anions; c) H-bond interactions between bis-amidinium cations and $\mathbf{1}H_2^{2-}$; d) various H-bond geometries exhibited in **HOF1**.

into the crystalline framework through photoinduced isomerisation. Although photoinduced isomerisation is unlikely to be pertinent to the crystallisation of **HOF2**, it is likely that the crystallisation process is aided by localised heating from the incident sunlight. However, we cannot rule out that photoexcitation of the NDI may contribute to the crystallisation process.

HOF2 crystallizes with one $\mathbf{3}^{5-}$ anion and two and a half bis-amidinium cations in the crystallographic asymmetric unit accompanied by multiple solvent molecules. It is known that imide groups are susceptible to ring-opening in the presence of base,[14] and **HOF2** exhibits this behaviour with one of the NDI imide rings opening to generate an additional carboxylate moiety (Fig. 4c), leading to charge-balance in the system. The intact phenyl imide moiety maintains an angle of 78.1° between the planes formed by the phenyl and naphthalene imide group, similar to the arrangement seen in the structure of $\mathbf{2(Et)_4}$. In **HOF2** the anion is fully deprotonated, unlike in **HOF1**. The components of the HOF are arranged in a 3D pillared structure, where the bis-amidinium is both involved in the formation of the sheet alongside the NDI-based anions, whilst also serving as a pillar between the layers of the sheet (Fig. 1b). The crystal structure of **HOF2** reveals that the phosphonate benzene ring in the closed imide ring sits perpendicularly to the NDI plane (83.7°), inhibiting close aggregation between adjacent molecules.

The anion in **HOF2**, $\mathbf{3}^{5-}$, is hydrogen-bonded to seven surrounding molecules: six bis-amidinium cations and one $\mathbf{3}^{5-}$ anion (Fig. 4c), affording a total of 13 H-bond interactions per anion. The two phosphonate groups are H-bonded to four neighbouring bis-amidinium molecules, forming parallel interactions with each of them (d_2a_2), with interaction distances

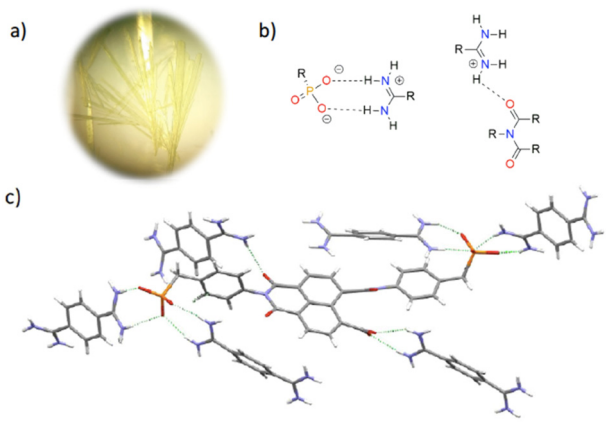

Fig. 4 **HOF2**: a) photographic image of yellow needle crystals of **HOF2**; b) the H-bond geometries exhibited in **HOF2**; c) interactions between $\mathbf{3}^{5-}$ anions and bis-amidinium cations in **HOF2**; note the ring-opened imide in the anionic tecton.

(P–O···H–N) ranging from 1.86 Å to 2.14 Å and ∠OHN 177.2° to 141.0°. One of the carbonyl groups of the closed ring interacts with a nearby amidinium, creating a weak single (d_1a_1) interaction (C═O···H–N, 2.16 Å, and ∠OHN 127.5°).

The stability of **HOF2** was examined by thermogravimetric analysis (TGA) and powder X-ray diffraction (PXRD). TGA measurements indicated that the network gradually released guest water molecules, up to *ca.* 85 °C, accounting for approximately 20% of the total weight of the sample (Fig. 5a). A sharp weight loss, attributed to the decomposition of bis-amidinium cations, is then observed above ~180 °C. The frameworks phase purity, crystallinity, and stability were evaluated using PXRD. A PXRD experiment was conducted on air-dried crystals without grinding, and the observed diffraction pattern was compared with the calculated pattern derived from the single crystal structure. Grinding of the sample results in significant peak broadening and loss of crystallinity. The stability of the framework after activating the sample under vacuum for two days was also assessed (Fig. 5b). The PXRD pattern obtained for this dried sample showed notable changes suggesting decomposition or a phase transition due to solvent removal.

Conclusions

In this study we have prepared amidinium···phosphonate based HOFs. In the case of tectons **1** and **3** the CH_2 group between benzene and phosphonate affords flexibility which we anticipate aids crystallization but potentially leads to close-packed, rather than porous, framework structures. Both **HOF1** and **HOF2** form potentially porous structures, but removal of water molecules leads to collapse of the framework structure. This observation suggests that the presence of hydrogen bonding water molecules is important to the integrity of HOFs. Notably in **HOF2** the NDI tecton, **3**, is sensitive to basic conditions, which results in the opening of one of the imide rings and a more complex tecton with additional hydrogen bond accepting sites, lowering the predictability of the synthetic strategy. The formation of **HOF2** is aided by sunlight which could be leading to localised heating of the crystallisation solution. The complications encountered during the synthesis of these HOFs leads to increased complexity of framework structure. Although phosphonate tectons readily form HOFs in combination with amidinium-based species, a diversity of interactions encountered between the anionic and cationic tectons presents significant challenges when seeking to prepare amidinium···phosphonate based frameworks.

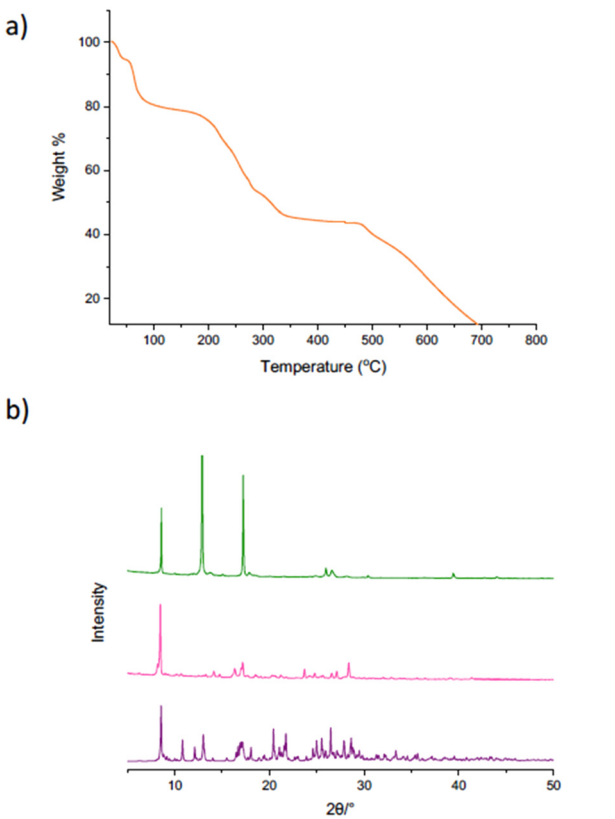

Fig. 5 a) Thermogravimetric analysis for **HOF2**; b) PXRD patterns recorded for **HOF2**: simulated (top – green), as synthesised (middle – pink), and dried sample (bottom – purple).

Experimental

Synthesis of 1 (biphenyl-4,4′-diphosphonic acid)

The synthesis of this compound was carried out according to literature procedures.[32]

Crystal data for $C_{14}H_{20}O_8P_2$ (M = 378.24 g mol^{-1}): monoclinic, space group $P21/c$ (no. 14), a = 14.8893(5) Å, b = 6.2149(2) Å, c = 9.0927(3) Å, $\alpha = \gamma = 90°$, β = 93.663(3)°, V = 839. 86(5) Å^3, Z = 2, T = 100.00(10) K, μ(Cu Kα) = 2.730 mm^{-1}, D_{calc} = 1.496 g cm^{-3}, 7416 reflections measured (5.95° ≤ 2θ ≤ 155.246°), 1792 unique (R_{int} = 0.0586) which were used in all calculations. The final R_1 was 0.04895 ($I > 2\sigma(I)$) and wR_2 was 0.1484 (all data).

Synthesis of HOF1

1 (12.3 mg, 0.036 mmol) was dissolved in H_2O (3.90 mL) and 1 M NaOH (0.1 mL). A solution of 1,4-phenyl-bis-amidinium dichloride (8.5 mg, 0.036 mmol), dissolved in H_2O (4 mL), was layered on top of the solution of **1**, followed by a third layer of MeOH. The layers were allowed to mix slowly. The reaction mixture vial was sealed in a vial and kept at room temperature. Within 2 days, a few colourless needle-like crystals formed. FT-IR (cm^{-1}): 2900 (w, br), 1662 (m), 1538 (m), 1496 (m), 1470 (m), 1243 (m), 1195 (m), 1126 (m), 1060 (s), 912 (s), 856 (m), 817 (m), 719 (m), 693 (m), 615 (w), 589 (m), 553 (m), 519 (s), 414 (w), 464 (s).

Crystal data for $C_{22}H_{26}N_4O_6P_2$ (M = 504.41 g mol^{-1}): monoclinic, space group $C2/c$ (no. 15), a = 12.0665(2) Å, b = 13.6291(3) Å, c = 15.2147(2) Å, $\alpha = \gamma = 90°$, β = 92.9890(10)°, V = 2498.74(8) Å^3, Z = 4, T = 100.02(16) K, μ(Cu Kα) = 2.062 mm^{-1}, D_{calc} = 1.341 g cm^{-3}, 11 250 reflections measured, 2643 unique (R_{int} = 0.0494) which were used in all calculations. The final R_1 was 0.1162 ($I > 2\sigma(I)$) and wR_2 was 0.2245 (all data).

Synthesis of *N*,*N*′-di(4-benzylphosphonic acid diethyl ester) 1,4,5,8-naphthalenetetracarboxylic diimide (2)

The synthesis of this compound was carried out according to a literature procedure with some minor modifications.[33] Full details are described in ESI.†

Crystal data for $C_{36}H_{36}N_2O_{10}P_2$ (M = 359.30 g mol^{-1}): monoclinic, space group $P2_1/n$ (no. 14), a = 5.51236(3) Å, b = 15.23409(8) Å, c = 19.29148(11) Å, $\alpha = \gamma = 90°$, β = 97.9423(6)°, V = 1604.478(15) Å^3, Z = 2, T = 100.02(16) K, μ(Cu Kα) = 1.796 mm^{-1}, D_{calc} = 1.487 g cm^{-3}, 27 458 reflections measured, 3248 unique (R_{int} = 0.0191) which were used in all calculations. The final R_1 was 0.0303 ($I > 2\sigma(I)$) and wR_2 was 0.0802 (all data).

N,*N*′-Di(4-benzylphosphonic acid) 1,4,5,8-naphthalenetetra carboxylic diimide (3)

The synthesis of this compound was carried out according to a literature procedure with some minor modifications.[34] A flame-dried two-neck flask was purged three times with N_2 and charged with **2** (0.500 g, 0.70 mmol) in anhydrous CH_2Cl_2 (8 mL). The solution was cooled to 0 °C and trimethylsilyl bromide (1 mL, 6.8 mmol) was added dropwise, under a nitrogen atmosphere. The reaction mixture was stirred for 40 minutes at 0 °C, allowed to warm to RT, and stirred for a further 48 h. Solvent was removed by rotary evaporation, then MeOH (40 mL) was added to the residue and stirred at room temperature for 4 hours. The crude product was filtered under reduced pressure and washed with methanol, yielding H_6PNDI (**3**) as a light yellow powder (0.39 g; yield 93%). MS (MALDI-TOF) m/z [M]$^-$: 606.06. ^{1}H NMR (400 MHz, DMSO-d_6) δ (ppm): 8.72 (s, 4H), 7.43 (dd, J = 8.4, 2.3 Hz, 4H), 7.36 (d, J = 8.2 Hz, 4H), 3.10 (s, 2H), 3.03 (s, 2H). ^{13}C NMR (101 MHz, DMSO-d_6) δ (ppm): 163.50, 133.69, 133.14, 131.61, 131.00, 130.93, 128.98, 127.46, 31.15, 30.64. ^{31}P NMR (162 MHz, DMSO-d_6) δ (ppm): 20.55.

Synthesis of HOF2

3 (14 mg, 0.023 mmol) was dissolved in H_2O (3.90 mL) and 1 M NaOH (0.1 mL) in a vial. A solution of 1,4-phenyl-bis-amidinium dichloride (8 mg, 0.034 mmol), dissolved in H_2O (4 mL), was layered on top of the solution of **3**. The reaction mixture vial was sealed and kept at room temperature near an external window. Within 5 hours, yellow needle-like crystals formed. Yield (24%).

Crystal data for $C_{28}H_{16}N_2O_{11}P_2{\cdot}2.5(C_8H_{12}N_4)$ (M = 1028.91 g mol^{-1}): triclinic, space group $P\bar{1}$ (no. 2), a = 10.7489(1) Å, b = 11.1092(1) Å, c = 28.1083(2) Å, α = 92.980(1)°, β = 92.563(1)°, γ = 102.701(1)°, V = 3264.47(5) Å^3, Z = 2, T = 100.15 K, μ(CuKα) = 1.448 mm^{-1}, D_{calc} = 1.413 g cm^{-3}, 117 847 reflections measured, 13 490 unique (R_{int} = 0.0431) which were used in all calculations. The final R_1 was 0.0923 ($I > 2\sigma(I)$) and wR_2 was 0.2732 (all data).

Data availability

The X-ray crystallographic coordinates for structures reported in this study have been deposited at The Cambridge Crystallographic Data Centre (CCDC), under deposition numbers 2352949–2352952. These data can be obtained free of charge from The Cambridge Crystallographic Data Centre *via* **https://www.ccdc.cam.ac.uk/structures**.

Conflicts of interest

There are no conflicts to declare.

Acknowledgements

N. R. C. gratefully acknowledges support from the UK Engineering and Physical Sciences Research Council (EP/S002995/2). A. R. Y. A. gratefully acknowledges the support provided by King Faisal University. We acknowledge the EPSRC UK National Crystallography Service at the University of Southampton for the collection of crystallographic data.

Notes and references

1 C. Aakeröy, N. R. Champness and C. Janiak, *CrystEngComm*, 2010, **12**, 22–43.
2 A. G. Slater, L. M. A. Perdigao, P. H. Beton and N. R. Champness, *Acc. Chem. Res.*, 2014, **47**, 3417–3427.
3 I. Hisaki, C. Xin, K. Takahashi and T. Nakamura, *Angew. Chem., Int. Ed.*, 2019, **58**, 11160–11170.
4 B. Wang, R.-B. Lin, Z. Zhang, S. Xiang and B. Chen, *J. Am. Chem. Soc.*, 2020, **142**, 14399–14416.
5 Y. Wang, C. Wang, D. Wang, G. Zhuang, K. O. Kirlikovali, P. Li and O. K. Farha, *J. Am. Chem. Soc.*, 2022, **144**, 10663–10687.
6 L. Chen, B. Zhang, L. Chen, H. Liu, Y. Hu and S. Qiao, *Mater. Adv.*, 2022, **3**, 3680–3708.
7 W. Yang, A. Greenaway, X. Lin, R. Matsuda, A. J. Blake, C. Wilson, W. Lewis, P. Hubberstey, S. Kitagawa, N. R. Champness and M. Schröder, *J. Am. Chem. Soc.*, 2010, **132**, 14457–14469.
8 J. D. Wuest, *Chem. Commun.*, 2005, 5830–5837.
9 P. Dechambenoit, S. Ferlay, N. Kyritsakas and M. W. Hosseini, *J. Am. Chem. Soc.*, 2008, **50**, 17106–17113.
10 M. D. Ward, *Chem. Commun.*, 2005, 5838–5842.
11 N. G. White, *Chem. Commun.*, 2021, **57**, 10998–11008.
12 P. Muang-Non, A. W. Markwell-Heys, C. J. Doonan and N. G. White, *Chem. Commun.*, 2023, **59**, 4059–4062.
13 J. Nicks, S. A. Boer, N. G. White and J. A. Foster, *Chem. Sci.*, 2021, **12**, 3322–3327.
14 A. R. Y. Almuhana, G. R. F. Orton, C. Rosenberg and N. R. Champness, *Chem. Commun.*, 2024, **60**, 452–455.
15 S. Lie, T. Maris and J. D. Wuest, *Cryst. Growth Des.*, 2014, **14**, 3658–3666.
16 S. Zheng, L. Li, L. Chen, Z. Fan, F. Xiang, Y. Yang, Z. Zhang and S. Xiang, *Z. Anorg. Allg. Chem.*, 2022, **648**, e202200031.
17 E. M. Fatila, M. Pink, E. B. Twum, J. A. Karty and A. H. Flood, *Chem. Sci.*, 2018, **9**, 2863–2872.

18 W. Zhao, B. Qiao, J. Tropp, M. Pink, J. D. Azoulay and A. H. Flood, *J. Am. Chem. Soc.*, 2019, **141**, 4980–4989.
19 B. K. Tripuramallu and S. K. Das, *J. Solid State Chem.*, 2013, **197**, 499–507.
20 J.-W. Zhang, C.-C. Zhao, Y.-P. Zhao, H.-Q. Xu, Z.-Y. Du, H.-L. Jiang, B. K. Tripuramallu and S. K. Das, *CrystEngComm*, 2013, **197**, 499–507.
21 T. Zeng, L. Wang, L. Feng, H. Xu, Q. Cheng and Z. Pan, *Dalton Trans.*, 2019, **48**, 523–534.
22 K. Krekić, D. Klintuch and R. Pietschnig, *Chem. Commun.*, 2017, **53**, 11076–11079.
23 J.-W. Zhang, C.-C. Zhao, Y.-P. Zhao, H.-Q. Xu, Z.-Y. Du and H.-L. Jiang, *CrystEngComm*, 2014, **16**, 6635–6644.
24 C. B. Aakeröy, A. M. Beatty, B. A. Helfrich and M. Nieuwenhuyzen, *Cryst. Growth Des.*, 2003, **3**, 159–165.
25 H. Zhao, Z. Zhou, X. Feng, C. Liu, H. Wu, W. Zhou and H. Wang, *Nano Res.*, 2023, **16**, 8809–8816.
26 Q.-H. Ling, J.-L. Zhu, Y. Qin and L. Xu, *Mater. Chem. Front.*, 2020, **4**, 3176–3189.
27 F. Würthner, C. R. Saha-Möller, B. Fimmel, S. Ogi, P. Leowanawat and D. Schmidt, *Chem. Rev.*, 2015, **116**, 962–1052.
28 P.-W. Yi, W.-H. Chiu, T. Kudo, T. Sugiyama, R. Bresoli-Obach, J. Hofkens, E. Chatani, R. Yasukuni, Y. Hosokawa and S. Toyouchi, *J. Phys. Chem. C*, 2021, **125**, 18988–18999.
29 K. Yuyama, T. Sugiyama and H. Masuhara, *J. Phys. Chem. Lett.*, 2013, **4**, 2436–2440.
30 S. Shin, F. Menk, Y. Kim, J. Lim, K. Char, R. Zentel and T.-L. Choi, *J. Am. Chem. Soc.*, 2018, **140**, 6088–6094.
31 P. Muang-Non, H. D. Toop, C. J. Doonan and N. G. White, *Chem. Commun.*, 2022, **58**, 306–309.
32 Z. Wang, J. M. Heising and A. Clearfield, *J. Am. Chem. Soc.*, 2003, **125**, 10375–10383.
33 K. P. Nandre, S. V. Bhosale, K. V. S. Rama Krishna, A. Gupta and S. V. Bhosale, *Chem. Commun.*, 2013, **49**, 5444–5446.
34 B. Shan, A. Nayak, M. K. Brennaman, M. Liu, S. L. Marquard, M. S. Eberhart and T. J. Meyer, *J. Am. Chem. Soc.*, 2018, **140**, 6493–6500.

